

Seismic behavior of steel reinforced concrete (SRC) joints with new-type section steel under cyclic loading

Qiuwei Wang*, Qingxuan Shi and Hehe Tian

College of Civil Engineering, Xi'an University of Architecture and Technology, Xi'an, P.R. China

(Received December 03, 2014, Revised March 13, 2015, Accepted June 29, 2015)

Abstract. No significant improvement has been observed on the seismic performance of the ordinary steel reinforced concrete (SRC) columns compared with the reinforced concrete (RC) columns mainly because I, H or core cross-shaped steel cannot provide sufficient confinement for core concrete. Two improved SRC columns by constructing with new-type section steel were put forward on this background: a cross-shaped steel whose flanges are in contact with concrete cover by extending the geometry of webs, and a rotated cross-shaped steel whose webs coincide with diagonal line of the column's section. The advantages of new-type SRC columns have been proved theoretically and experimentally, while construction measures and seismic behavior remain unclear when the new-type columns are joined onto SRC beams. Seismic behavior of SRC joints with new-type section steel were experimentally investigated by testing 5 specimens subjected to low reversed cyclic loading, mainly including the failure patterns, hysteretic loops, skeleton curves, energy dissipation capacity, strength and stiffness degradation and ductility. Effects of steel shape, load angle and construction measures on seismic behavior of joints were also analyzed. The test results indicate that the new-type joints display shear failure pattern under seismic loading, and steel and concrete of core region could bear larger load and tend to be stable although the specimens are close to failure. The hysteretic curves of new-type joints are plumper whose equivalent viscous damping coefficients and ductility factors are over 0.38 and 3.2 respectively, and this illustrates the energy dissipation capacity and deformation ability of new-type SRC joints are better than that of ordinary ones with shear failure. Bearing capacity and ductility of new-type joints are superior when the diagonal cross-shaped steel is contained and beams are orthogonal to columns, and the two construction measures proposed have little effect on the seismic behavior of joints.

Keywords: steel reinforced concrete (SRC) beam-column joint; cross-shaped steel with flanges; arranging along diagonal line; quasi-static test; shear failure; seismic behavior

1. Introduction

During the past few decades, steel reinforced concrete (SRC) structural systems have been used in many tall buildings all over the world. This system combines the rigidity and formability of reinforced concrete with the strength and speed of construction associated with structural steel to produce an economic structure. The concrete used for encasing structure steel section not only increase its strength and stiffness but also improve its fire-resistance. The seismic behavior of SRC

*Corresponding author, Associate Professor, E-mail: wqw0815@126.com

members and its influence factors have been studied by many researchers abroad (Tanaka *et al.* 2000, Yasushi *et al.* 2004, Joao and Rodrigo 2005, Minae and Koichi 2008, Shim *et al.* 2008, Sav *et al.* 2011, Kim *et al.* 2011, Karimi *et al.* 2012, Kian *et al.* 2012). From the early 1990s, with the wide use of SRC structures in China, many Chinese scholars began to do some research on the seismic behavior of SRC columns (Jiang and Jia 2007, Chen *et al.* 2009, Guo *et al.* 2010, Zhang *et al.* 2012, Zheng *et al.* 2012, Chen *et al.* 2014, Lu *et al.* 2014). The results have shown that SRC columns embedded with I, H or core cross-shaped steel were mainly adopted in the engineering practice while these ordinary section steel could provide limited confinement for core concrete, and no significant improvement has been observed on the seismic behavior of the ordinary SRC columns compared with the reinforced concrete (RC) columns. So, it has become more essential to develop new SRC structures to promote the earthquake resistance, the workability and economy.

Two improved SRC columns embedded with new-type section steel are developed in the study to overcome the shortcomings of ordinary SRC columns on this background. The first type is a cross-shaped steel whose flanges are in contact with concrete cover (short for “enlarging cross-shaped steel”), and the second type is a rotated cross-shaped steel whose webs coincide with diagonal line of the column’s sections (short for “diagonal cross-shaped steel”). Completed experimental studies have shown that the seismic behavior of new-type SRC columns is better than that of ordinary ones when other conditions are same (Wang *et al.* 2013). The strength and ductility of new-type columns are better than that of ordinary ones by theoretical analysis, which is attributed to increased area of confined concrete because of appearance of the two cross-shaped steel arrangements. This phenomenon could be explained from two aspects which are respectively the strength and area of confined concrete.

Firstly, lateral pressure loads provided by steel and stirrup are evenly distributed in confined concrete when the SRC column is under the ultimate state. There are many studies on strength and ductility of restrained reinforced concrete members, and the strength formula of confined concrete by Mander *et al.* (1988) is adopted as Eq. (1).

$$f_{cc} = f_c \left(-1.254 - 2 \frac{f_1}{f_c} + 2.254 \sqrt{1 + \frac{7.94 f_1}{f_c}} \right) \quad (1)$$

Where f_{cc} is confined concrete compressive strength; f_c is unconfined concrete compressive strength; and f_1 is the effective lateral confining stress (see Mander *et al.* 1988).

And then, the lateral confinement on the concrete core could be divided into strong constraint and weak constraint, which are respectively provided by steel and stirrup. Based on the theories of the confined concrete (Chung *et al.* 2002), the concrete area under strong confinement condition for new-type SRC columns is larger than that for the ordinary column, and this is because concrete area confined by steel is proportional to that surrounded by steel. For weak confinement condition, the confined concrete area of ordinary and new SRC columns is basically same.

Beam-column joints in a composite structural system consisting of reinforced or confined concrete columns and composite beams are crucial zones for effective transfer of forces between the connecting elements in structures and significantly affect the seismic performance of composite structural system. Detailed experimental studies of composite beam-column joints for buildings in seismic regions have been undertaken in the last several decades by Nishiyama *et al.* (2004), Morino and Kawaguchi (2005), Chou and Uang (2007), Wang *et al.* (2010), Ma *et al.* (2011), Fan *et al.* (2014), Chen *et al.* (2015) and Liu *et al.* (2015). Many types of connection details were examined, including connections for concrete-filled steel tubular (CFST) column and

H-shaped steel beams, connections for SRC column and composite steel-concrete beams, connections for H-shaped steel column and steel beams, connections for reinforced concrete column and composite steel-concrete beams, and connections for H-shaped steel column and steel beams, and it has been observed that composite beam-column joints, reasonably designed, demonstrate good ductility and energy dissipation capacity under earthquake loads.

However, as compared with the above joints, connections for SRC column and SRC beams are seldom studied, and most of existing research work has been performed mainly on ordinary SRC joints, i.e., the SRC beam and columns embedded with conventional section steel (I, H or core cross-shaped steel). The advantages of new-type columns have been proved theoretically and experimentally, yet when the new-type SRC columns are jointed onto SRC beams with I-shaped steel, the construction measures and seismic behavior of the beam-column joints remain unclear. And thus, it is necessary to investigate the seismic behavior of this kind of new-type SRC joints. Moreover, in the previously discussed experimental research, the specimens were primarily designed to have such strong joint region that the connection damages often occurred at the beam ends, although the joint region remained elastic. As a result, the mechanical behavior of the joint region was not reflected in the experimental results.

This study investigated the mechanical behavior of connections between new-type columns and SRC beams with I-shaped steel. The steel skeletons embedded in the beam and column were welded together to transfer the bending moment effectively, and the construction measures were designed according to Chinese specification JGJ 138 (Design code 2001). Tests of five specimens under low reversed cyclic loading were conducted, and test results were evaluated in terms of hysteretic characteristics, energy dissipation capacity, strength and stiffness degradation, joint ductility and shear deformation. Additional investigations focused on the effects of steel shape, load angel and construction measures on the mechanical behavior of connections.

2. Experimental program

2.1 Describe of specimens

To force the joint damage to occur at the joint region, rather than at the beam ends as most existing joint experiments have demonstrated, the beams and columns of the specimens were designed to have approximately equal flexural strength. This differs from current design codes for structures. The test presented in this study consisted of totally five SRC beam-column joints, named as SSRCJ1~SSRCJ5 respectively. The enlarging cross-shaped steel with flanges was

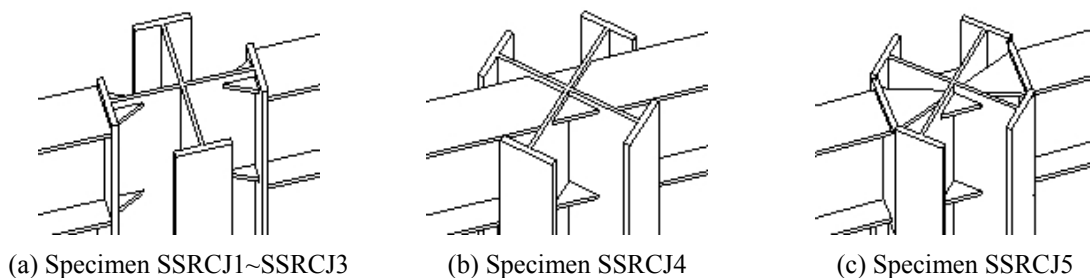


Fig. 1 The connection forms of steel skeletons

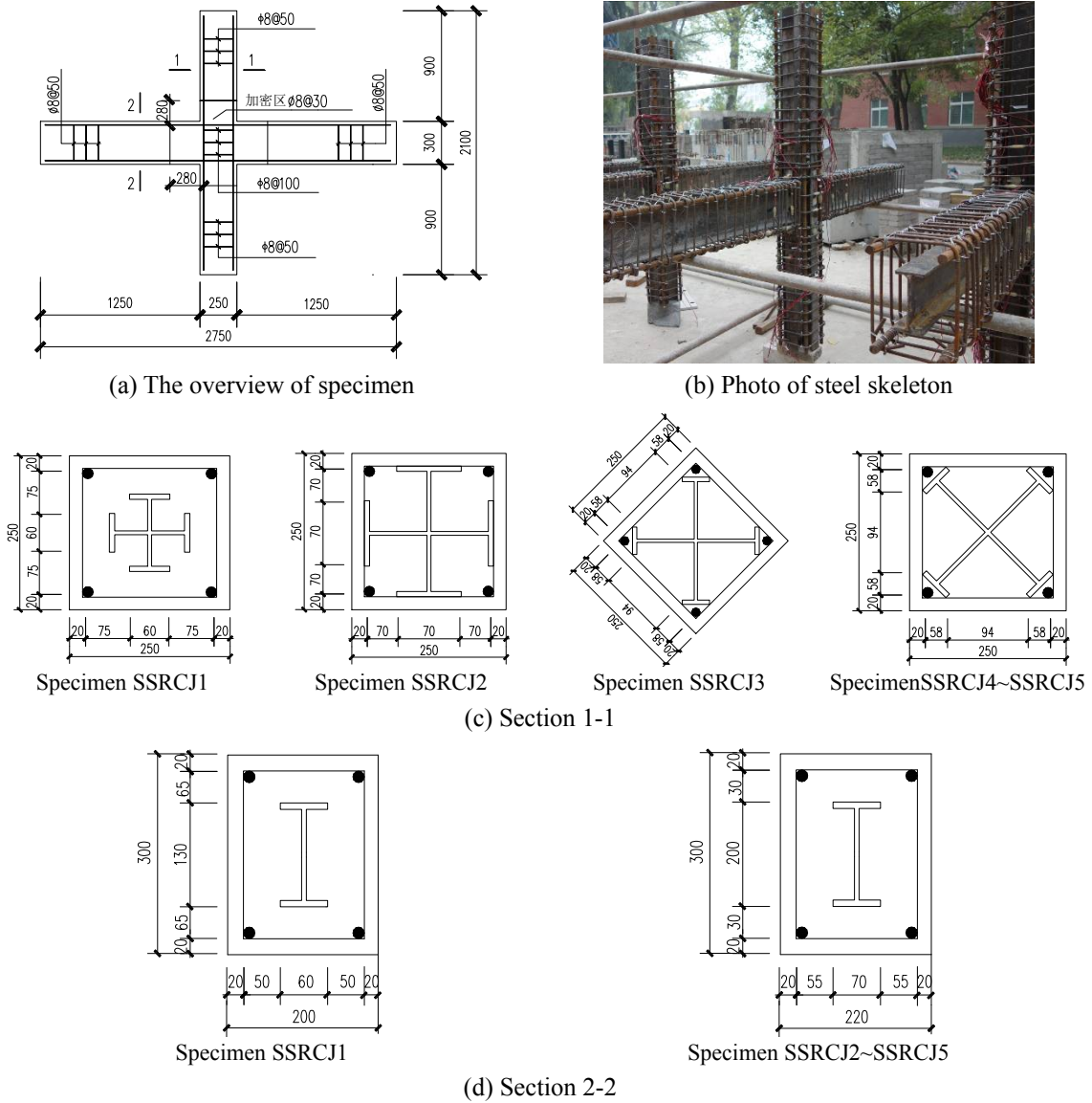


Fig. 2 Geometry and steel arrangement of specimens

adopted for the column of specimen SSRCJ2, and the diagonal one for columns of specimens SSRCJ3~SSRCJ5. Unlike the other specimens, the beam was oblique to the column for the specimen SSRCJ3. An ordinary SRC beam-column joint (SSRCJ1) as control specimen was test for comparison, for which core cross-shaped steel was embedded in the column. The common hot-rolled I-shaped steel was used for beams of SRC joints. The connection forms of steel skeletons are shown in Fig. 1. Dimensions and reinforcement arrangement of all specimens are illustrated in Fig. 2.

In order to satisfy the requirements of building function and structural arrangement, the beams are usually needed to be oblique to the columns, and this is the design background of the specimen

Table 1 Specimen sectional dimensions

Specimen	Steel in the column		Steel in the beam		Axial compression ratio n_t
	Steel section $h_w \times b_f \times h_f \times t_w$ (mm ⁴)	Steel ratio (%)	Steel section $h_w \times b_f \times h_f \times t_w$ (mm ⁴)	Steel ratio (%)	
SSRCJ1	130×60×6×8	6.20	130×60×6×8	3.14	
SSRCJ2	194×70×5×8	7.09	200×70×5×8	3.31	
SSRCJ3	210×70×5×8	7.39	200×70×5×8	3.31	0.40
SSRCJ4	210×70×5×8	7.39	200×70×5×8	3.31	
SSRCJ5	210×70×5×8	7.39	200×70×5×8	3.31	

* $h_w \times b_f \times h_f \times t_w$: b_f and h_f are the flange width and height, and h_w and t_w are the web height and thickness respectively;

* n_t : The axial compression ratio is calculated according to the formula $n_t = N_k / (f_{ck}A_c + f_{ak}A_a)$. Where N_k is the applied axial compression force; f_{ck} and A_c are the standard values of compressive strength and cross sectional area for concrete; f_{ak} and A_a are respectively the standard values of tensile strength and cross sectional area for steel.

SSRCJ3. Oblique layout here means that the beam sits at a 45-degree angle to the axial line of column section in a plane.

In all test specimens, the columns were 2100-mm-high with cross section of 250 mm×250 mm and the beams were 2750-mm-long with cross section of 200 mm×300 mm (SSRCJ1) and 220 mm×300 mm (SSRCJ2~SSRCJ5). The concrete used in the specimens was C50, the embedded steel was Q235, the longitudinal reinforcement was HRB400 with 20 mm diameter, and the stirrup was HPB300 with 6mm diameter. The concrete cover thickness was 20 mm, and stirrup spacing for the encrypted region, low density zone and joint core area were respectively 30 mm, 50 mm and 100 mm. Different parameters were involved in these specimens to investigate the influences on the seismic behavior of SRC joints, including the steel shape, load angel and construction measures. Table 1 collects the details of the tested specimens.

The steel was cut and machined according to design requirements. In order to ensure the stress transfer of beam-column joints, several holes were opened on the steel web of columns as channels of longitudinal reinforcement in beams because the steel and reinforcement bars intersected for specimens SSRCJ2~SSRCJ5. Then the longitudinal reinforcement was settled by tying with stirrup to form a reinforced skeleton frame, and formwork support and pouring concrete could be completed on this basis.

2.2 Material properties

Material strength used to evaluate ultimate stress uses the result of the material test. The mechanical properties of steel, longitudinal reinforcement and stirrup from test are listed in Table 2. C50 commercial pumping concrete was adopted, and concrete pouring for all the specimens was finished as the same batch. The six reserved standard cube specimens (150×150×150 mm³) were tested before test and the strength index for every concrete sample is shown as Table 3. The mean concrete compression strength of standard cube specimens is 51.2 MPa.

Table 2 Material properties of steel

Material	Grade	Yield strength f_y (MPa)	Ultimate strength f_u (MPa)	Elastic modulus E (MPa)
Steel	Q235 (5 mm thick)	248.3	388.8	2.0×10^5
	Q235 (6 mm thick)	245.5	395.6	2.0×10^5
	Q235 (8 mm thick)	230.6	388.0	2.0×10^5
Longitudinal reinforcement	HRB400	448.1	613.4	2.0×10^5
Stirrup	HPB300	309.5	480.7	1.7×10^5

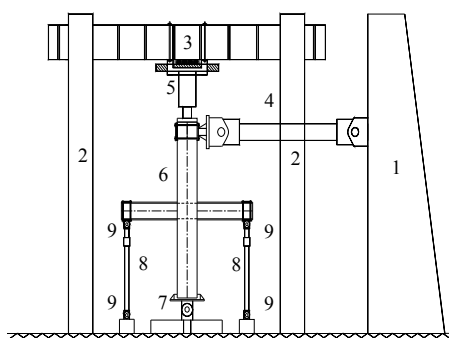
Table 3 Strength index of concrete samples

Concrete samples	1	2	3	4	5	6
Test values of cube compressive strength f_{cu} (MPa)	55.8	52.7	46.7	52.5	48.9	50.7

2.3 Test setup and loading history

A schematic view of the loading apparatus is shown in Fig. 3. Columns were pin-connected at their ends to present inflection points at the midspan of the member length. The pinned connection at the bottom of the column was achieved by using a three dimensional spherical plain bearing made specifically for this experiment. The vertical load was applied on the top of column using hydraulic actuators.

There were two loading steps in the test, as follows: (1) an axial compression force was firstly induced by a load-jack (in accordance with the target axial compression ratio) and maintained constant during the whole course of loading; and (2) a reversed cyclic load was then applied laterally using a MTS actuator (servo-controlled hydraulic type). In the phase before specimen yielding, lateral loading was triggered by increments of force. The first level of the force was 20% of the calculated capacity of the specimens P_{u-cal} and 10% of P_{u-cal} was gradually increased on the



(a) Sketch map



(b) Photo of the actual load

1. reaction wall; 2. reaction steel frame; 3. reaction girder; 4. actuator for lateral force;
5. oil jack; 6. test specimen; 7. column hinge device; 8. sensors; 9. beam hinge device

Fig. 3 The test setup

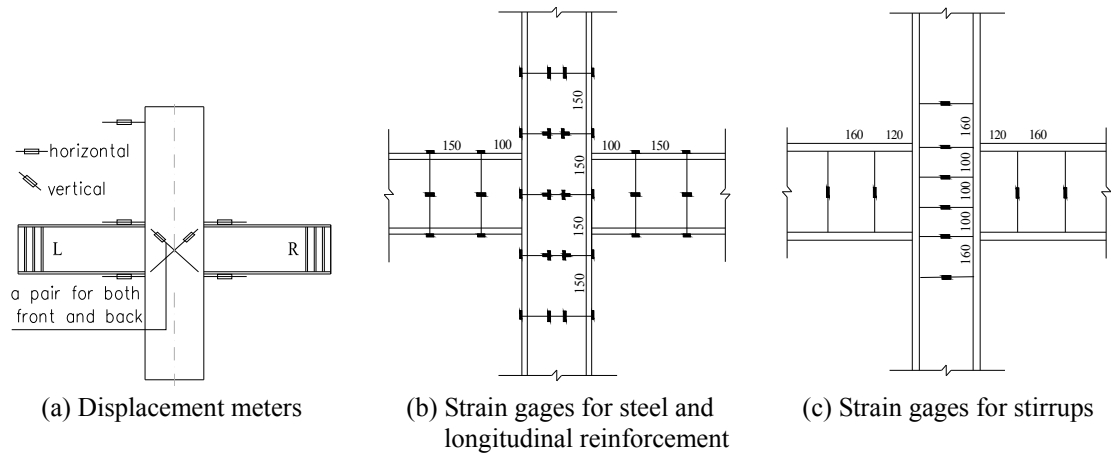


Fig. 4 Measurement points arrangement of specimens

next levels. On every force level, the lateral load was repeated only once. While after specimen yielding, lateral loading was triggered by increments of displacement. The yielding displacement Δ_y was gradually increased on the next displacement level and the lateral load was repeated three times on every level, where Δ_y is the calculated lateral displacement of the column when the steel flange yields. The test was stopped until the lateral load reduced to 85% of the ultimate load or the column couldn't keep its stability.

During the test, the lateral load in addition to the displacement and the strain of the steel, reinforcement and stirrup were measured and recorded automatically. The lateral load is measured by the sensor installed on the actuator and the lateral displacement is measured by displacement meters on top of the specimens. The joint shear deformation is measured by two pairs of crossed displacement meters in core area. The main measuring point arrangement is shown in Fig. 4. It's important to note that, displacement meters cannot be set in the joint core region along the diagonal direction for the specimen SSRCJ3, and so the Fig. 4(a) is only for specimens SSRCJ1~SSRCJ2 and SSRCJ4~SSRCJ5.

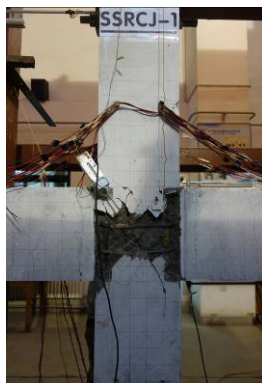
3. General behavior and failure pattern

The shear failure of joint core was occurred for all specimens in general. Fig. 5 shows the final failure pattern of specimens SSRCJ1~SSRCJ5 under low reversed cyclic loading. The shear deformation was small and no cracks appeared on the specimen at the preliminary stage of loading, and the horizontal displacement and steel strain increased with the increasing load in a linear relation. During the 40 kN load step in the force control stage, the first vertical crack was developed at the beam ends whose length and distance from the edges of the column were respectively 50~100 mm and 50~80 mm. With the load increasing, the new vertical cracks appeared in succession at the beam ends and the first vertical crack extended to the joint core area. During the 80~90 kN load step, cracks were appeared in joint core regions whose direction were parallel to the diagonal line, and cracks along the diagonal direction were afterwards developed on the other side of specimens at the 130~140 kN load step.

At the stage of displacement-controlled, it was observed that new diagonal cracks in the joint

core regions were developed and the existing diagonal cracks were constantly broadening by which the joint core concrete were divided into diamond blocks, however, there was no significant increase for vertical cracks at the beam ends. During the $1\Delta_y$ load step, the main diagonal crack run through the joint core area and steel web in the column began to yield from part to whole. At this stage, the strain of stirrups in the joint core area increased faster while only a few reached its yield value, and the strain of steel flange was very small which had much effect to confine joint core concrete. During the $2\Delta_y$ load step, the crossing cracks extended to the column body below the node and the steel web and stirrup gradually yielded, by contrast, the strain of steel and bars at ends of the beam and column remained basically stable. During the final load step ($3\Delta_y$), the panel shear deformation increased significantly and the stirrup completely yielded, and then the encased concrete was crushed and exposed. At the final stage of the load test, the specimens were seriously damaged because of losing strength and stiffness.

There were three loading phase during the whole course of the tests which were elastic, elastic-plastic and plastic stages respectively. Apart from the specimen SSRCJ1, there was a rising trend in the applied lateral load for other specimens because the concrete area confined by steel in the joint is larger, following the initial decrease. The failure phenomena were slightly different for new SRC beam-column joints due to the effect of steel shape, load angle and construction



(a) Specimen SSRCJ1



(b) Specimen SSRCJ2



(c) Specimen SSRCJ3



(d) Specimen SSRCJ4



(e) Specimen SSRCJ5

Fig. 5 Failure modes of specimens

measures. Part of joint core concrete was still complete until the specimen was damaged for specimen SSRCJ2. The concrete outside of steel flange in the column was so less that the initial crack firstly appeared here, which then extended towards joint core regions for specimens SSRCJ4 and SSRCJ5. The beam was oblique to the column for specimen SSRCJ3 whose joint zone includes beam ends and column edges, and diagonal cracks appeared firstly at beam ends in the joint region and then extended to column edges when the specimen was close to yield.

Generally, the decline rate of the bearing capacity and stiffness for new-type SRC joints (SSRCJ2~SSRCJ5) was lower than that of the ordinary one (SSRCJ1) on every force and displacement level, and concrete confined by steel of core region could bear larger load and tend to be stable although the specimens were close to failure. This illustrates that the proposed new-type SRC joints have better seismic ductility and higher earthquake energy dissipation capacity.

4. Experimental results and discussion

4.1 Hysteretic characteristics

The hysteretic curve is an important basis to determine the seismic performance. The relationship between the applied lateral load and displacement for all specimens are shown in Fig. 6, and the following characteristics could be drawn through analysis.

- (1) The specimens behave approximately elastic before the horizontal load increases to the yield load (about 40% of the ultimate load). The stiffness of the specimens decreases slowly from the yield load to the ultimate load and the plastic deformation is small. It is clear that the hysteretic curves start to fall after the ultimate load for all specimens. However, it exhibits a positive ductility as the displacement dramatically develops with smaller loss of load-bearing capacity.
- (2) The hysteretic loops of the specimens are plump except specimen SSRCJ1 during the elastoplastic range. There are long level or decline segments after peak value in the envelope curves for new-type joints (SSRCJ2~SSRCJ5), reflecting a strong capacity of plastic deformation and energy dissipation. Meanwhile, the new-type joints have larger bearing capacity and deformation ability even after the failure load.
- (3) The area of hysteretic loop for the specimen SSRCJ1 is smaller than that of specimens SSRCJ2~SSRCJ5 whose strength and stiffness degradation are more serious, illustrating that the energy dissipation of new-type joints is better with high axial compression ratio. The reasons for this phenomenon are mainly summed up into two aspects: one is that enlargement of both area and moment of inertia in new-type section steel is obvious comparing with core cross-shaped steel; and the other is that enlarging or diagonal cross-shaped steel with flanges could provide larger confinement for concrete in the joint. The seismic behavior of specimens SSRCJ2~SSRCJ5 is thus improved.
- (4) The steel shape and construction measures are different for specimens SSRCJ2~SSRCJ5, but there are no significant differences for their hysteretic loops. The reason is that the steel content and confined concrete area in the beam and column are almost equal for the four specimens.

4.2 Skeleton curves

A skeleton curve can be obtained by connecting the peak points of the hysteretic curves under

every level of load. A skeleton curve is used to observe the deformation capacity and strength decay of specimens. Fig. 7 shows the skeleton curves of the test specimens, where P and Δ are respectively the horizontal load and displacement. Four observations can be made, as follows:

- (1) The loading process of all specimens could be divided into elastic, elastic-plastic and plastic stages, but there is no obvious yield point on the skeleton curves. The main reason is that the yield of steel web in the joint core region has its progressive development of the process from part to whole. Compared with the ordinary SRC joints, the new-type SRC joints have better ductility and energy dissipation whose descent part of skeleton curves is smoother.
- (2) The beam is respectively orthogonal and oblique to the column for specimens SSRCJ2 and SSRCJ3 although their connection forms of steel skeleton are the same. The peak load of the specimen SSRCJ3 is higher than that of the specimen SSRCJ2, while strength and stiffness degradation of the former is more obvious and serious.
- (3) The steel shape and steel content are the same for specimens SSRCJ4 and SSRCJ5

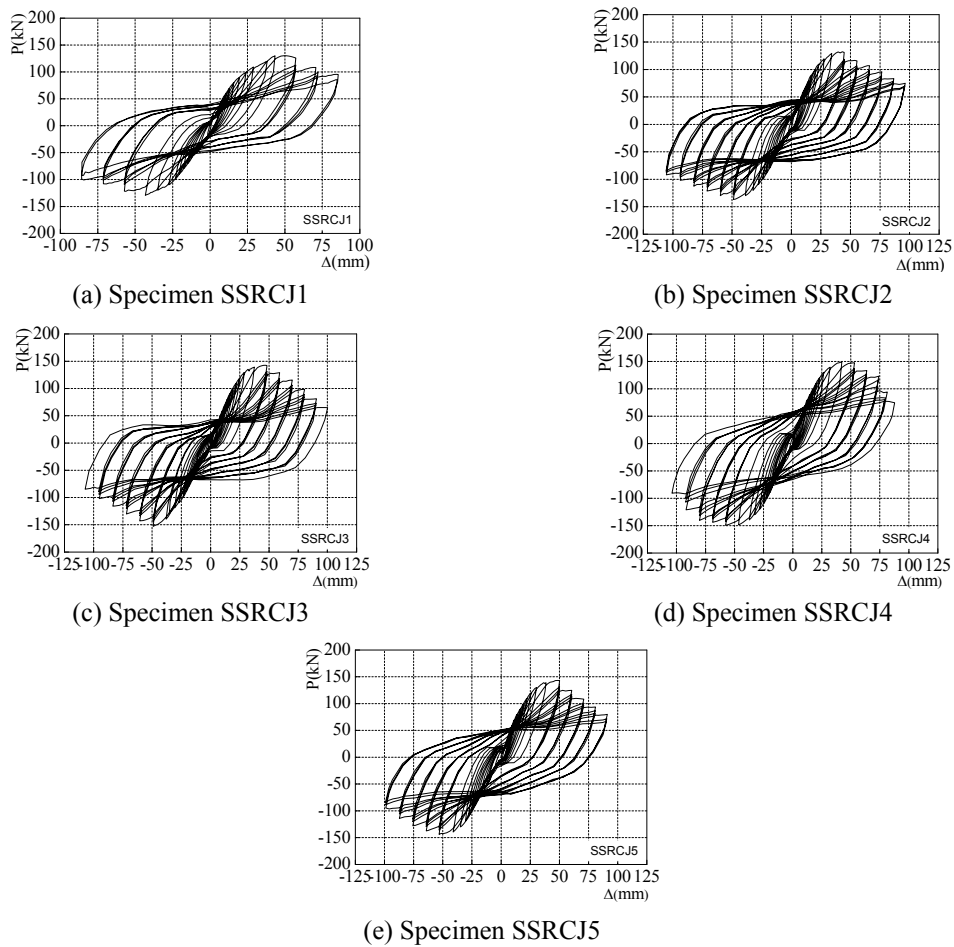


Fig. 6 The hysteretic curves

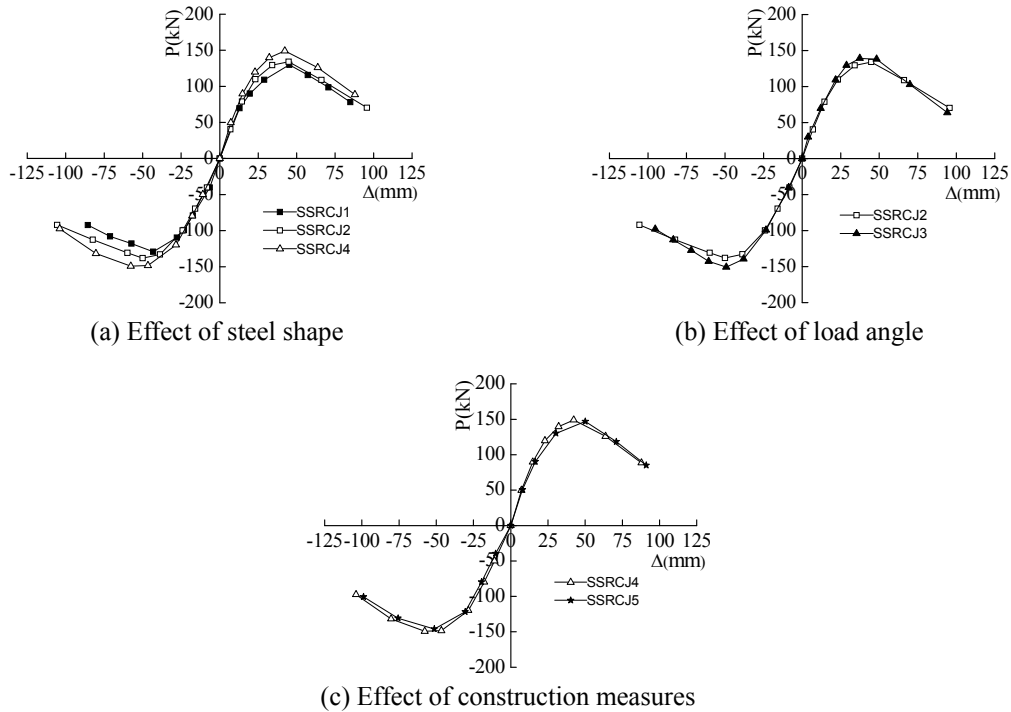


Fig. 7 The skeleton curves

although their construction measures are different. The steel in the beam and column is connected by directly welding for specimen SSRCJ4 but by diaphragm plates for the specimen SSRCJ5. The shape and the major feature points (such as the peak load and limit displacement) of skeleton curves are similar for the two specimens, and it can be concluded that seismic behavior of the new-type joints are approximately the same when the two construction measures proposed are used.

- (4) The bearing capacity and deformation properties of the specimen SSRCJ2 are lower than specimens SSRCJ4 and SSRCJ5 while saving about 5% steel content. Seismic behavior of SRC joints is generally superior when the diagonal cross-shaped steel with flanges is contained.

4.3 Energy dissipation capacity

Energy dissipation capacity is an important seismic performance index for structure, which is usually represented by equivalent viscous damping coefficient h_e . By analyzing the hysteretic loops of test specimens under low cyclic reversed loading, the degree of energy dissipation under different loading level can be investigated. The equivalent viscous damping coefficient can be defined as follows

$$h_e = \frac{1}{2\pi} \cdot \frac{S_{ABCD}}{S_{OBE} + S_{ODF}} \tag{2}$$

Where S_{ABCD} and $(S_{OBE}+S_{ODF})$ are the area of hysteretic loop ABCD and shadowed areas within

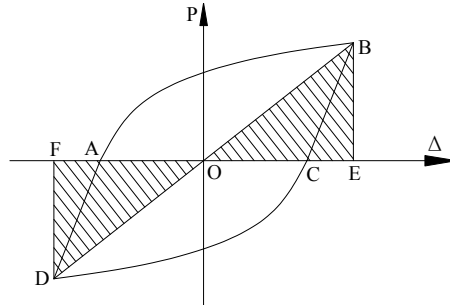
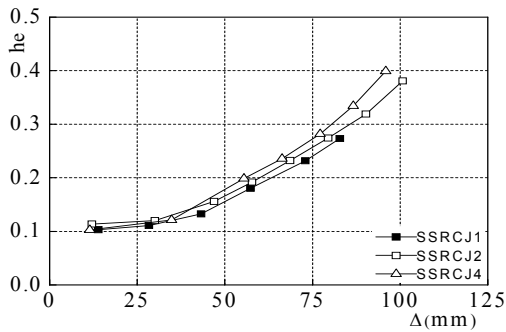


Fig. 8 The calculation of equivalent viscous damping coefficient

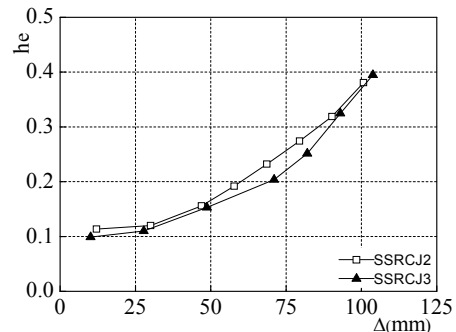
the triangles OBE and ODF respectively, as shown in Fig. 8.

The increase of the equivalent viscous damping coefficient (h_e) with displacement (Δ) is shown in Fig. 9. The values of h_e are about 0.40 for specimens SSRCJ2~SSRCJ5 and drop to 0.28 for the specimen SSRCJ1 with the same axial compression ratio, indicating that energy dissipation capacity of new-type SRC joints are greater than that of the ordinary ones.

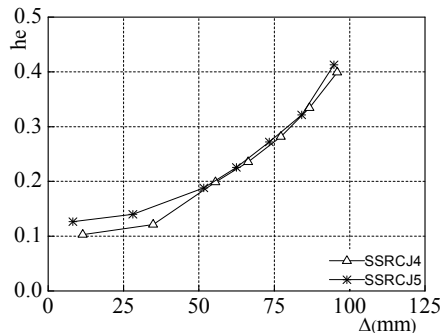
Moreover, it can be seen from Fig. 9 that (1) h_e from specimen SSRCJ2 is larger than that from specimen SSRCJ3. It may reflect that the orthogonal specimen has higher energy dissipation capacity comparing with the oblique crossing specimen when their steel content differs little;



(a) Effect of steel shape



(b) Effect of load angle



(c) Effect of construction measures

Fig. 9 Equivalent viscous damping coefficients

(2) h_e from specimens SSRCJ4 and SSRCJ5 are larger than other specimens on the same displacement level, indicating that the specimens with diagonal cross-shaped steel show higher earthquake energy dissipation capacity; and (3) compared comprehensively, h_e from the specimen SSRCJ4 is larger than that from the specimen SSRCJ5, and it can be inferred that the force transmission is more direct for the construction measure adopted by the specimen SSRCJ4.

4.4 Strength degradation curves

The strength degradation of SRC beam-column joints can be denoted by deteriorated coefficient λ_j which means the ratio between the peak load of every period and the first period on the same displacement level. Fig. 10 shows the degradation of joint strength with the peak displacement in each load step. The results show that λ_j of all specimens generally decreases with increased displacement, and the reason is that the concrete deterioration and steel yield lead to the decline of bearing capacity. Except the specimen SSRCJ1, attenuation amplitude of the strength is smaller for other specimens whose hysteretic curves are approximately rhombic in shape.

Comparising between specimens SSRCJ2 and SSRCJ3, the strength attenuation is rapid for the latter and slowly for the former, and thus oblique layout for SRC joints accelerates attenuation rate of bearing capacity. In addition, the decrease of bearing capacity is less for specimens SSRCJ4 and SSRCJ5 in the first three or four cycle whose λ_j reduces to 0.85 in the last cycle, reflecting that construction measures have some effect on the strength degradation and bearing capacity of new-type joints with the diagonal cross-shaped steel is superior.

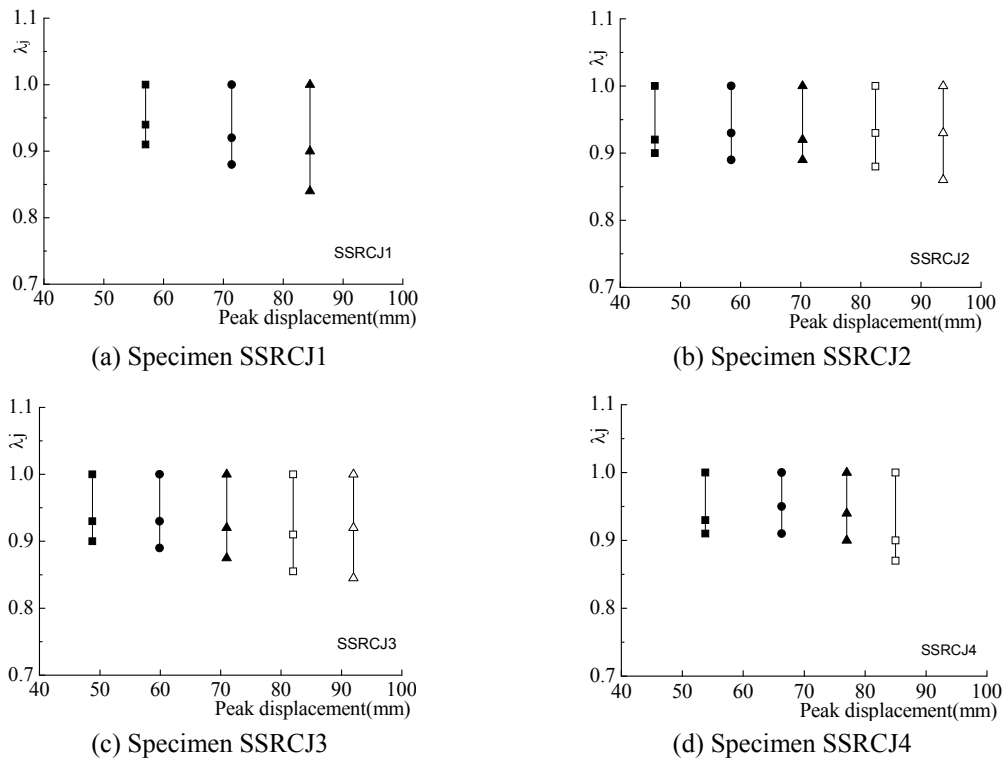
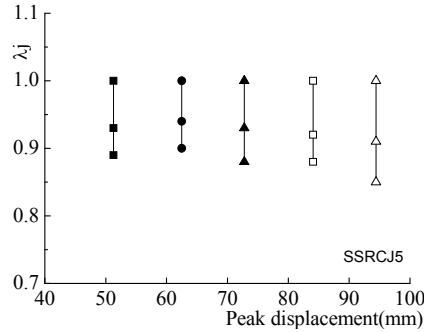
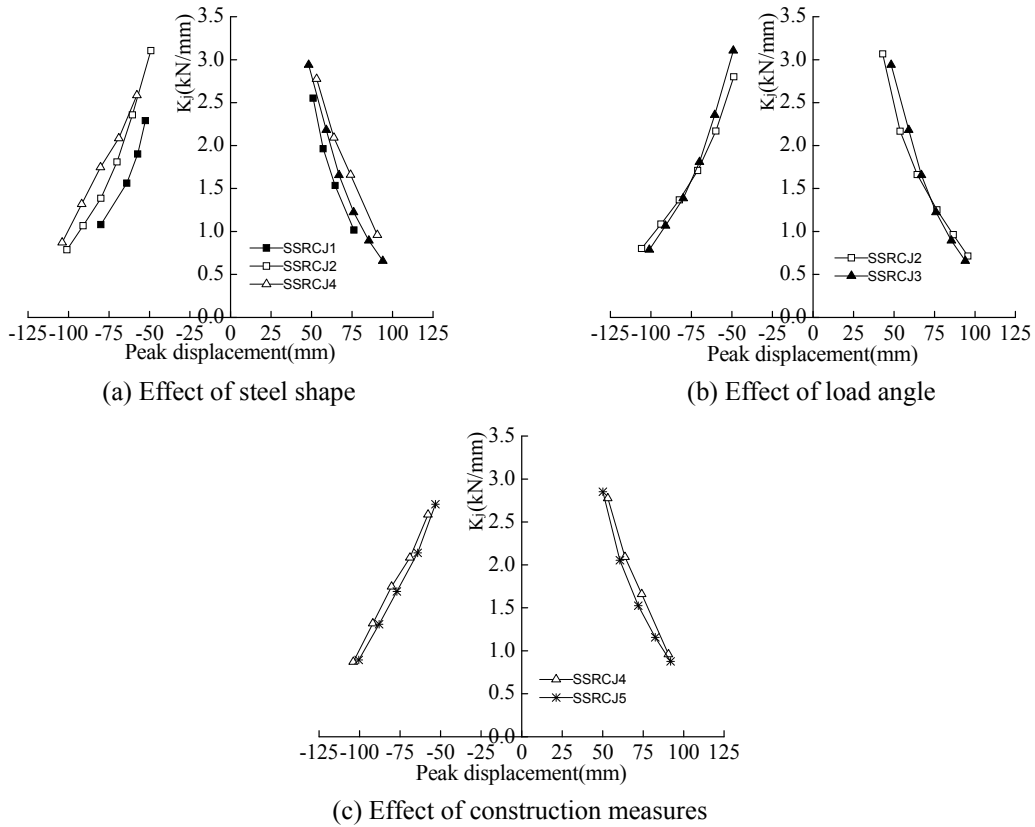


Fig. 10 The strength degradation curves



(e) Specimen SSRCJ5

Fig. 10 Continued



(a) Effect of steel shape
 (b) Effect of load angle
 (c) Effect of construction measures
 Fig. 11 The rigidity degradation curves

4.5 Stiffness degradation curves

The stiffness degradation reflects the degradation of the resistance of lateral collapse. The stiffness of the test specimen under low cyclic reversed loading can be expressed in secant stiffness. The secant stiffness is the ratio of peak load in every load level and the associated

displacements in displacements in positive and negative direction. Fig. 11 shows the degradation of joint stiffness degradation with the load step, where the x-axis represents the peak displacement of each load step, and y-axis represents the secant stiffness K_j under different loading level.

The figure clearly shows that (1) stiffness degradation curves of the specimens change steadily, and it grows fast in prime period of load and then slows down to over 0.5 gradually. The reason lies in that the joint core concrete is confined by steel and the stiffness degradation rate become slow at the later loading stage; (2) the stiffness degradation of the specimen SSRCJ1 is the most serious because the ordinary core cross-shaped steel was embedded, which makes concrete area confined by steel in the joint be smaller. By comparison, the stiffness degradation rate is obvious improved for specimens SSRCJ2~SSRCJ5, reflecting that it makes less loss of vertical bearing capacity for new-type joints with the same storey drift ratio; and (3) among the new-type SRC joints, the degree of stiffness degradation for specimens SSRCJ3 and SSRCJ4 are respectively the maximal and the minimal. The reason can be summed up into two aspects. One is that the confinement effect is more obvious at the later loading stage, and the stiffness is steady for the specimen with diagonal cross-shaped steel. The other is that the oblique crossing specimen has the problem of stress concentration, and steel flange with increasing strain in the joint core has less confinement effect for concrete which intensifies the phenomenon of stiffness degradation.

4.6 Deformation and ductility performance

Ductility is used to determine the deformation capacity and seismic behavior of structural members. The ductility factor μ , defined as the ratio of the ultimate displacement Δ_u to the yield displacement Δ_y , is usually used to quantitatively describe the ductility. Where Δ_y is calculated using the Park method (Park 1989), and Δ_u is the corresponding displacement as the horizontal load decreases to 85% of the ultimate load. Table 4 shows the ductility factors of all specimens.

It can be seen from Table 4 that Δ_u and μ of the ordinary SRC joint (SSRCJ1) are respectively 1/35 and 2.45, while corresponding values for new-type SRC joints (SSRCJ2~SSRCJ5) are over 1/30 and 3.2~4.1. It can be concluded that the ductility performance of new-type SRC joints is much better than ordinary ones under the same conditions. The steel shape and load angel have greater influence on the ductility performance of SRC joints, which may be presented as the three following aspects.

- (1) The Δ_u and μ of specimens SSRCJ4 and SSRCJ5 are improved by 18% than that of the specimen SSRCJ2 when other conditions are same, reflecting that the deformation capacity and ductility performance of SRC joints with diagonal cross-shaped steel are

Table 4 Ductility factors of specimens

Specimen	Yield displacement Δ_y (mm)		Ultimate displacement Δ_u (mm)		Ultimate drift ratio θ_u	Ductility factor μ
	Positive	Negative	Positive	Negative		
SSRCJ1	24.87	-25.02	60.53	-61.86	1/35	2.45
SSRCJ2	22.02	-24.55	74.10	-76.65	1/28	3.24
SSRCJ3	23.15	-25.43	69.88	-72.12	1/30	2.99
SSRCJ4	19.68	-23.92	75.36	-91.89	1/25	4.09
SSRCJ5	18.43	-20.34	72.74	-79.70	1/27	3.93

more superior. The reason is that the flange and web of diagonal cross-shaped steel can bear load along the two non-orthogonal directions, and force decomposition can increase the area of joint core concrete confined by steel.

- (2) The specimen SSRCJ2 has a more improvement in ductility factor μ over the specimen SSRCJ3, and the deformation property of oblique specimen (SSRCJ3) is 7% lower than the orthogonal one (SSRCJ2) by analyzing quantization calculation. It can be deduced from above that the oblique specimens may well be used in the practical engineering when designed and implemented properly.
- (3) The Δ_u and μ of the specimens SSRCJ4 and SSRCJ5 are closer, showing that the two construction measures proposed have little effect on the seismic behavior of joints. From the construction point of view, the steel skeleton embedded in the specimen SSRCJ4 has better general performance and less welding seam which is much easier to be constructed than the specimen SSRCJ5.

4.7 The joint shear deformation

The shear angle γ is adopted to measure the shear deformation of connection core. The rectangular section denotes the joint core area in the measuring range, as shown in Fig. 12. The joints extend $|\delta_1 + \delta_2|$ in one direction and shorten $|\delta_3 + \delta_4|$ in the other direction under shear loading. Therefore, the average strain in diagonal direction can be calculated as follows

$$\bar{X} = \frac{|\delta_1 + \delta_2| + |\delta_3 + \delta_4|}{2} \quad (3)$$

and

$$\sin \theta = \frac{b}{\sqrt{h^2 + b^2}}, \quad \cos \theta = \frac{h}{\sqrt{h^2 + b^2}}, \quad \alpha_1 = \frac{\bar{X} \sin \theta}{h}, \quad \alpha_2 = \frac{\bar{X} \cos \theta}{b} \quad (4)$$

therefore

$$\gamma = \alpha_1 + \alpha_2 = \frac{\bar{X} \sin \theta}{h} + \frac{\bar{X} \cos \theta}{b} = \frac{\bar{X}}{hb} \left[\frac{h^2 + b^2}{\sqrt{h^2 + b^2}} \right] = \frac{\sqrt{h^2 + b^2}}{hb} \bar{X} \quad (5)$$

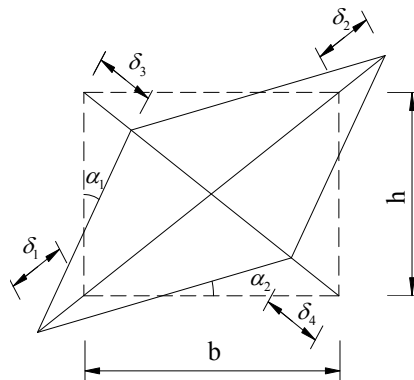


Fig. 12 Shear deformation of connection core

Where b and h are the sizes of joint core regions, namely the column width and the beam height

respectively.

The relationship between the shear force (V) and shear angle (γ) can be obtained through Eqs. (3)-(5), as shown in Fig. 13. It is important to note that, the beam is oblique to the column for the specimen SSRCJ3 and crossed displacement meters cannot be guaranteed to be set in the joint core region, and thus shear deformation of the specimen SSRCJ3 has not been presented. In addition, the ultimate shear angle is denoted by the deformation angle corresponding to 0.92 times peak shear stress, and the reason lies in that spalling of concrete cover for joint core area is serious at the later loading stage and the ultimate shear angle could not be measured by dial indicator.

It can be seen from Fig. 13 that the shear angle increases linearly with the shear force in the initial stage. The curves are becoming nonlinear with the increase of the cyclic number, and more irrecoverable deformation is presented. This shows that the joints are mainly at phase of elastic-plasticity which agrees with the shear failure pattern.

Meanwhile, it can be seen that (1) the negative shear angle of the ordinary SRC joint (SSRCJ1) is slightly larger than that of other specimens with the load increasing, reflecting that the cross-shaped steel could provide stronger confinement which makes the shear deformation of joints be smaller; and (2) the shear angle of specimens SSRCJ4 and SSRCJ5 is larger comparing with other joints, and thus shear deformation of joints embedded with the diagonal cross-shaped steel is more obvious.

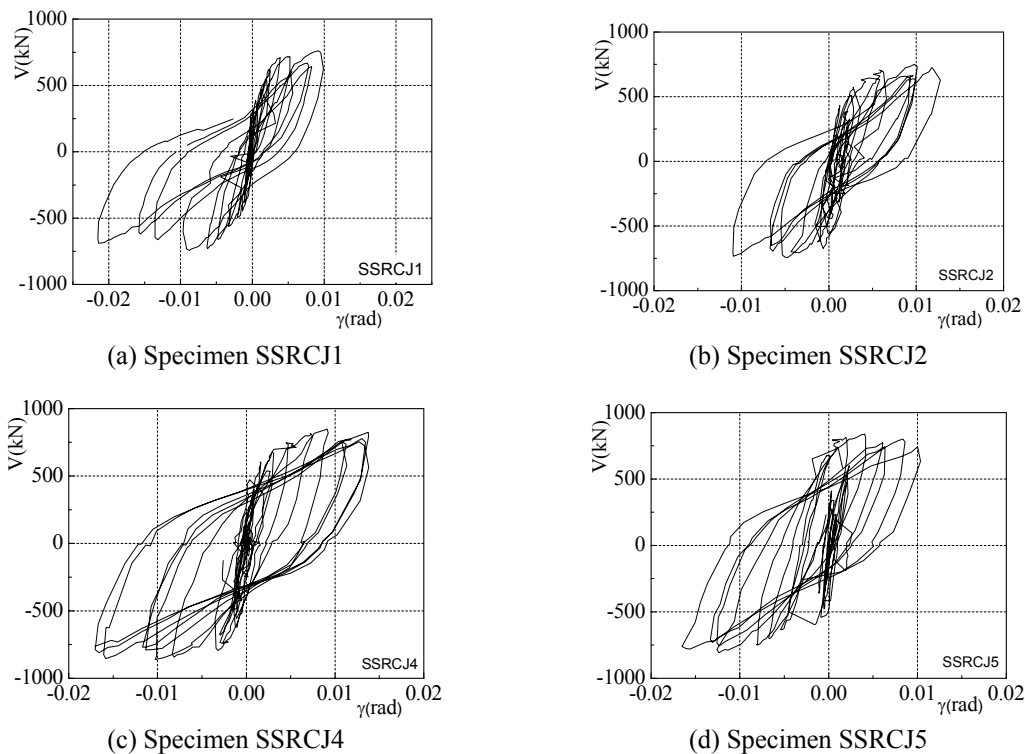


Fig. 13 Shear force (V) versus shear transformation (γ) curves

4.8 The design recommendation and in-situ application

Based on above analysis, the conclusion can be drawn that the new-type SRC joints have better seismic behavior than the ordinary one. While in the actual projects, how would a designer go about choosing the proposed new-type SRC joints?

For this question, the following design recommendations can be offered for reference: (1) 7%~9% steel ratio of the column is more reasonable for new-type SRC beam-column joints, because the joint could meet the demands for carrying capacity and ductility with this steel content. A larger content will lead to a certain waste of steel, on the contrary, will decrease the deformation capacity to some degree; (2) for the multi-story composite structures, it is recommended to choose the SRC joint embedded with *I*, H-shaped or core cross-shaped section steel, while for the high-rise building structures, it is necessary to choose new-type SRC joints due to higher vertical load; (3) among the SRC joints embedded with enlarging and diagonal cross-shaped steel, the seismic behavior of the latter is a bit better, while the former could save about 5% steel and be convenient to be constructed. So the designers can decide which one to choose based upon their own demands.

5. Conclusions

Through the experiments on the seismic behavior of four new-type and one contrastive SRC joint specimens under low reversed cyclic loading, some conclusions are drawn, as follows:

- The SRC beam-column joint specimens display shear failure mode and the shear deformation at failure is obvious under seismic load. Although the specimens are close to failure, the new-type SRC joints could bear larger load and keep better stability than the ordinary one under the high vertical load. This indicates that the new-type SRC joints have the capacity of bearing load and resisting collapse at the elastic-plastic stage.
- The hysteretic curves of the new-type SRC joints are in plump shapes and have no significant pinch phenomenon, and the degeneration of bearing capacity is slow with the increase of the displacement. For new-type SRC joints, the ultimate drift ratio and the ductility factor are greater than 1/30 and 2.95 respectively, and the equivalent viscous damping coefficient is also larger than 0.35; while for the ordinary one, values of the three indexes are only 1/35, 2.45 and 0.28. It proves that the improved SRC joints exhibit better capacity of deformation and energy dissipation than the ordinary one with shear failure.
- The steel arrangement is an important factor that affects the seismic behavior of SRC beam-column joints. Under the same conditions, both the load capacity and deformation ability of SRC joints embedded with enlarging and diagonal cross-shaped steel are larger than that embedded with core cross-shaped steel, and the average increasing rate is 10.2% and 31.1% for the two aspects. Thus the mechanical properties of new-type SRC joints have a marked improvement over that of the ordinary one, and the new-type joints embedded with diagonal cross-shaped steel have better seismic behavior than that with enlarging cross-shaped steel.
- The load angle also affects the seismic behavior of SRC joints. The seismic behavior of the oblique specimens is slightly poorer than that of the orthogonal specimens, but better than that of the ordinary one. So it is a fact that the oblique specimens can be used normally while designing properly.
- For the SRC joints embedded with diagonal cross-shaped steel, the two proposed

construction measures (adopted in specimens SSRCJ4 and SSRCJ5) have little effect on the seismic behavior of specimens. And by contrast, the construction measures adopted by the specimen SSRCJ4 will be easier to be cut and machined from the point of construction.

Acknowledgments

The research described in this paper was supported by Program for Changjiang Scholars and Innovative Research Team in University (PCSIRT13089) and by the National Natural Science Foundation of China (No. 51178380 and No. 51108370). This support is sincerely appreciated.

References

- Chen, X.G., Mu, Z.G. and Zhang, J.B. (2009), "Experimental study on the seismic behavior of steel reinforced concrete columns", *J. Univ. Sci. Technol.*, **31**(12), 1516-1524. [In Chinese]
- Chen, C.H., Wang, C.K. and Sun, H.Z. (2014), "Experimental study on seismic behavior of full encased steel-concrete composite columns", *J. Struct. Eng.*, **140**(6), 1-10.
- Chen, Z.P., Xu, J.J., Chen, Y.L. and Xue, J.Y. (2015), "Seismic behavior of steel reinforced concrete (SRC) T-shaped column-beam planar and 3D hybrid joints under cyclic loads", *Earthq. Struct.*, **8**(3), 555-572.
- Chou, C.C. and Uang, C.M. (2007), "Effects of continuity plate and transverse reinforcement on cyclic behavior of SRC moment connections", *J. Struct. Eng.*, **133**(1), 96-104.
- Chung, H.S., Yang, K.H. and Lee, Y.H. (2002), "Stress-strain curve of laterally confined concrete", *Eng. Struct.*, **24**(9), 1153-1163.
- Design code (2001), Technical specification for steel reinforced concrete, JGJ138-2001, Beijing, China.
- Fan, J.S., Li, Q.W., Nie, J.G. and Zhou, H. (2014), "Experimental study on the seismic performance of 3D joints between concrete-filled square steel tubular columns and composite beams", *J. Struct. Eng.*, **140**(12), 1-13.
- Guo, Z.X., Lin, H. and Liu, Y. (2010), "Experimental study on seismic behavior of SRC columns with different stirrup configuration", *J. Build. Struct.*, **31**(4), 110-115. [In Chinese]
- Jiang, R. and Jia, J.Q. (2007), "Seismic ductility of very-high strength-concrete short columns subject to combined axial loading and cyclic lateral loading", *J. Chongqing Univ. (English Edition)*, **6**(3), 205-212.
- Joao, B.M. and Rodrigo, B.C. (2005), "Numerical analysis of composite steel-concrete column of arbitrary cross section", *J. Struct. Eng.*, **131**(11), 1721-1730.
- Karimi, K., El-Dakhkhni, W. and Tait, M. (2012), "Behavior of slender steel-concrete composite columns wrapped with FRP jackets", *J. Perform. Construct. Facil.*, **26**(5), 590-599.
- Kian, K., Wael, W. and Michael, J. (2012), "Behavior of slender steel-concrete composite columns wrapped with FRP jackets", *J. Perf. Cons. Fac.*, **26**(5), 590-599.
- Kim, S.H., Jung, C.Y. and Ann, J.H. (2011), "Ultimate strength of composite structure with different degrees of shear connection", *Steel Compos. Struct., Int. J.*, **11**(5), 375-390.
- Liu, Z.Q., Xue, J.Y., Peng, X.N. and Gao, L. (2015), "Cyclic test for beam-to-column abnormal joints in steel moment-resisting frames", *Steel Compos. Struct., Int. J.*, **18**(5), 1177-1195.
- Lu, X.L., Yin, X.W. and Jiang, H.J. (2014), "Experimental study on hysteretic properties of SRC columns with high steel ratio", *Steel Compos. Struct., Int. J.*, **17**(3), 287-303.
- Ma, H.W., Jiang, W.S. and Cho, C.D. (2011), "Experimental study on two types of new beam-to-column connections", *Steel Compos. Struct., Int. J.*, **11**(4), 291-305.
- Mander, J.B., Priestley, M.J.N. and Park, R. (1988), "Theoretical stress-strain model for confined concrete", *J. Struct. Eng.*, **114**(8), 1804-1826.
- Minae, F. and Koichi, M. (2008), "Seismic performance of new type steel-concrete composite structures considering characteristic both SRC and CFT structures", *Proceedings of 14th World Conference on*

- Earthquake Engineering*, Beijing, China, October.
- Morino, S. and Kawaguchi, J. (2005), "Research on and construction of the concrete-filled steel tube column system in Japan", *Int. J. Steel Struct.*, **5**(4), 277-298.
- Nishiyama, I., Fujimoto, T., Fukumoto, T. and Yoshioka, K. (2004), "Inelastic force-deformation response of joint shear panels in beam-column moment connections to concrete-filled tubes", *J. Struct. Eng.*, **130**(2), 244-252.
- Park, R. (1989), "Evaluation of ductility of structures and structural subassemblages from laboratory testing", *Bull. New Zealand Soc. Earthq. Eng.*, **22**(3), 155-166.
- Sav, V., Campian, C. and Senila, M. (2011), "Composite steel-concrete columns with high strength concrete versus normal strength concrete", *Civil Eng. Arch.*, **54**(1), 74-81.
- Shim, C.S., Chung, Y.S. and Han, J.H. (2008), "Cyclic response of concrete-encased composite columns with low steel ratio", *Proceedings of the Institution of Civil Engineers-Struct. Build.*, **161**(2), 77-89.
- Tanaka, Y., Kaneko, Y. and Yashiro, H. (2000), "Strengthening of reinforced concrete columns by central reinforcing steel element", *Proceedings of 12th World Conference on Earthquake Engineering*, Auckland, New Zealand, February.
- Wang, Q.W., Shi, Q.X., Jiang, W.S., Zhang, X.H., Hou, W. and Tian, Y. (2013), "Experimental study on seismic behavior of steel reinforced concrete columns with new-type cross sections", *J. Build. Struct.*, **34**(8), 18-24. [In Chinese]
- Wang, T.C., Zhang, X.H., Zhao, H.L. and Qi, J.W. (2010), "Experimental research on seismic behavior of exterior joints with specially shaped columns reinforced by fiber", *Ind. Construct.*, **40**(1), 46-50.
- Yasushi, N., Shigeyuki, T. and Nozomu, B. (2004), "Flexural behavior of steel reinforced concrete columns with T-shaped steel", *Proceedings of 13th World Conference on Earthquake Engineering*, Vancouver, B.C., Canada, August.
- Zhang, S.A., Zhao, Z.Z. and He, X.Q. (2012), "Flexural behavior of SRC columns under axial and bilateral loading", *Appl. Mech. Mater.*, **166**, 3383-3390.
- Zheng, S.S., Lou, H.J., Wang, X.F. and Li, Z.Q. (2012), "Study on displacement ductility coefficient of steel reinforced high-strength concrete column", *Adv. Mater. Res.*, **368**, 1097-1100.